STRATEGIES FOR MAPPING ICE ON MARS USING CRISM VNIR WAVELENGTHS. C. E. Viviano[1], S. L. Murchie[1], F. P. Seelos[1], K. D. Seelos[1], and S. F. A. Cartwright[1,2]. [1]Johns Hopkins University Applied Physics Laboratory <Christina.Viviano@jhuapl.edu>, [2]University of Nevada, Reno.

Introduction: Mapping the spatial and temporal variations in the distribution of CO_2 and H_2O ices in the seasonal caps on Mars can reveal cycling between surface and atmospheric volatile reservoirs and help to constrain models of physical processes of volatile condensation and sublimation. Previous studies that mapped these phases have utilized short-wave infrared (SWIR) light (1-4 µm) measured by CRISM and OMEGA, leveraging diagnostic features in this wavelength range. While often physically mixed, the contributions from the different ices can be discriminated by the broad 1.5µm absorption feature distinctive of crystalline H_2O ice, and the narrow 1.435µm absorption (asymmetric stretching overtone) feature in CO_2 ice spectra [1] (see examples, Fig. 1).

Previous Observations. Broad and repeating coverage from OMEGA revealed the seasonal cap recession to be a dynamic process, with ablating CO_2 retreating in spring, and H_2O frost ablating and recondensing in nearby cold areas, such that a band of H_2O frost "follows" the receding CO_2 [2]. CRISM VNIR+SWIR mapping at 180 m/pixel has incomplete coverage yet also shows a complex pattern of ablation and redeposition with dependence on specific geographic features [3]. Km-per-pixel temperature and albedo measurements by TES, MCS, and MARCI reveal considerable interannual variability in frost coverage particularly in the south related to geography and temperature [4, 5].

Motivation for VNIR ice detection: With the degradation and eventual loss of the CRISM cryocooling system, the instrument now operates in a visible to near-infrared (VNIR)-only mode (0.4-1.05 µm). With its 90- and 180-m/pixel VNIR hyperspectral mapping modes (MSV, HSV), ongoing acquisition of CRISM VNIR data of the poles could help to further constrain spatial and temporal variations in ices. With that in mind, this effort aims to investigate and parameterize spectral features unique to CO_2 and H_2O ices within only the CRISM VNIR wavelengths, and then validate ability to map the ices using the full VNIR+SWIR spectral range.

Effects of Dust: The strengths of ice absorption features are dependent upon the mean path length of photons within the ice, which is related to the distance between grain boundaries or fractures (e.g., 'grainsize'), and the density of scattering particles (inclusions of dust) within the ice. Extremely small quantities of dust have been shown to affect H_2O ice spectra, especially at VNIR wavelengths where it lowers albedo, particularly at wavelengths <0.7 µm; this effect is even more enhanced with larger ice grain size [6]. While previous investigations [e.g., 7] have observed minor bands at ~0.8, 0.9 and 1.02 µm in association with water ice in the VNIR, these features can disappear with <0.1% dust [6]. Similarly, mixing of small quantities of dust with CO_2 ice lowers albedo, particularly at wavelengths less than ~0.7 µm [8].

Methods: We extracted icy and non-icy spectra from over 30 CRISM targeted observations, including the set initially analyzed in [9] over the south polar cap, a targeted observation over Louth Crater in the north polar region, and several high-spectral resolution mapping strips (HSP) that cover a range of CO_2- and H_2O- bearing ices and ice/dust mixtures. Using averaged spectra from these scenes (Fig. 1), we identified spectral characteristics that could be leveraged by different VNIR-only band parameter combinations. These combinations of VNIR-only products were compared and validated using standard ice-related CRISM browse products [10] utilizing SWIR wavelengths (ICE and IC2), and extracted spectra from each scene.

Results: We have demonstrated that by using CRISM VNIR (0.4–1.05 µm) wavelengths alone, several key features of the spectra can be characterized due to the following phenomena: (1) relatively dust-free H_2O ice exhibits VNIR overtone absorptions, particularly at 1.02 µm (Fig. 1, purple arrow), and (2) even traces of dust mixed into CO_2 and H_2O ices create correlations between ferric band depths and spectral

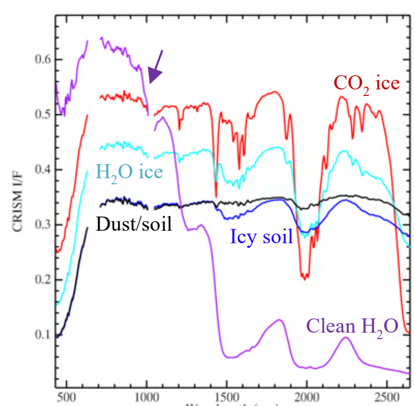

Figure 1. Average CRISM I/F spectra from targeted observations of CO_2 ice, H_2O-dominated ice, icy soils, and surrounding dust/soils within the scenes with little to no ice. Single spectrum (purple) of purer water ice with comparably less dust from Louth Crater (FRT00002F70). Purple arrow: water ice overtone at 1.02 µm near the VNIR and SWIR detector boundary indicated by the data gap.

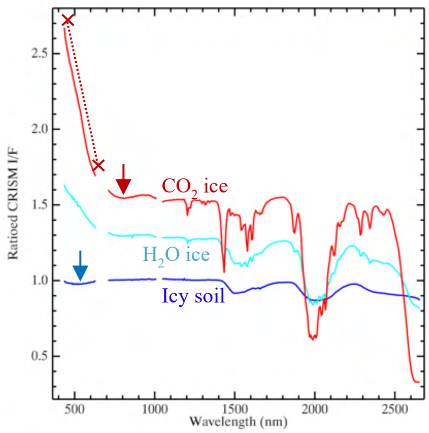

Figure 2. Spectra from Fig. 1 ratioed to the dust/soil spectrum (Fig. 1, black) to emphasize differences in VNIR features. Red arrow: 0.8-µm concavity present in CO2 ice. Blue arrow: 0.5-µm concavity strongest in H_2O ice bearing soils. Red dotted line: wavelengths used to calculate the red-blue ratio (RBR).

continua that are different from each other and from those in the surrounding martian regolith. Previous modeling of mixtures of martian dust with CO_2 ice [8] and H_2O ice [6] show that even 0.01% dust imparts a significant change to the VNIR. The effects of dust are consistent with an enhanced curvature of the spectrum around 0.5 µm (Fig. 2, blue arrow) for soils that contain water ice.

The standard CRISM summary parameter, BD530 (sensitive to nanophase ferric absorption) [10], can be used to highlight this feature. BD530 is stronger in H_2O-dominated ice signatures than in CO_2 ice, possibly due to a stronger contribution of dust in the H_2O ice, or differences in grainsize. Both H_2O and CO_2 ice-bearing materials also have a stronger negative slope than surrounding soils/dust, resulting in much lower RBR (red-blue ratio) values (Fig. 2, red dashed line). When compared to soil/dust, CO_2 ice also has a concave-upward shape near 800 nm that can be parameterized with a (new) third summary parameter, BD800 (Fig. 2, blue arrow). A fourth (new) summary parameter, D1020, measures the drop-off in reflectance at 1020 nm due to the H_2O ice absorption (Fig. 1, purple arrow).

Mapping of ices using VNIR data was tested on the over 30 CRISM observations using the four summary products described above, comparing results against ICE and IC2 (e.g., Fig. 3). A mask of RBR ≤ 3 is used to separate ice from soil. A useful new parameter composite, called 'ICV', for differentiating CO_2 ice from H_2O+CO_2 icy surfaces is shown in Fig 3: R: BD800, G: BD530_2, B: RBR. This new VNIR-only composite is comparable to SWIR images with a few caveats: 1) icy soil cannot be differentiated from dust/soil in the VNIR like it can in the SWIR (see Fig. 1, VNIR wavelengths); 2) CRISM data cannot be used to detect transparent CO_2 ice overlying soil by itself (i.e., cryptic terrain [4]) but thermal IR data from Mars Climate Sounder (MCS) could remove this ambiguity by detecting the low temperature of the CO_2 ice; 3) H_2O+CO_2 ice mixtures are not distinguishable from CO_2 ice using VNIR data alone, but MCS data would detect the low temperature of the CO_2 ice. While clean H_2O ice can be confused with CO_2 ice using the ICV browse product (Fig. 3), this ambiguity is resolved using D1020.

Conclusion: Leveraging several spectral features related to water ice and mixtures of dust with ices, we have demonstrated the ability to use the VNIR-only CRISM observations to detect and differentiate between CO_2 and H_2O ices, with the exception of icy soils and transparent CO_2 ice overlying soils.

Acknowledgements: This work was made possible through funding from the MRO Project to the CRISM team. All source data are publicly available on the PDS.

References: [1] Fink and Sill (1982), The infrared spectral properties of frozen volatiles, in *Comets*, 164–202. [2] Appéré, et al., (2011), *JGR*, 116(E05001). [3] Brown, et al. (2012), *JGR*, 117(E00J20). [4] Piqueux, et al. (2003), *JGR*, 108(E8). [5] Calvin, et al. (2017), *Icarus*, 292, 144-153. [6] Khuller et al. (2021), *JGR*, 126(9), e2021JE006910. [7] Dundas et al. (2018), *Science*, 359(6372), 199-201. [8] Singh and Flanner (2016), *JGR*, 121(10), 2037-2054. [9] Cartwright et al. (2021), LPSC 2021, Abs. #2169. [10] Viviano-Beck et al. (2014), *JGR*, 119(6), 1403-1431.

Figure 3. Three images with a 'true' visible image browse composite (TRU), a SWIR browse image (ICE, yellow/green=H_2O ice, magenta=CO_2 ice), and a new VNIR ice browse product (ICV), red/orange=CO_2 ice, green/blue=H_2O ice, black=icy soil or dust/soil.